Mon. Not. R. Astron. Soc. **000**, 1–3 (2011) Printed 25 August 2011 (MN LATEX style file v2.2)

The origin of cosmic-ray electrons in cluster outskirts

Anders Pinzke[1⋆], Peng Oh[1⋆], and Christoph Pfrommer[2⋆]
[1]*University of California - Santa Barbara, Department of Physics, CA 93106-9530, USA*
[2]*Heidelberg Institute for Theoretical Studies (HITS), Schloss-Wolfsbrunnenweg 33, DE - 69118 Heidelberg, Germany*

25 August 2011

ABSTRACT
bla bla bla

Key words: magnetic fields, cosmic rays, radiation mechanisms: non-thermal, elementary particles, galaxies: cluster: general

1 INTRODUCTION

2 SIMULATIONS

Our simulations were performed in a ΛCDM universe using the cosmological parameters: $\Omega_\mathrm{m} = \Omega_\mathrm{DM} + \Omega_\mathrm{b} = 0.3$, $\Omega_\mathrm{b} = 0.039$, $\Omega_\Lambda = 0.7$, $h = 0.7$, $n_\mathrm{s} = 1$, and $\sigma_8 = 0.9$. The total matter density in units of the critical density of the universe ρ_crit is denoted by Ω_m, the baryonic density by Ω_b, the DM density by Ω_DM and the cosmological constant today is denoted by Ω_Λ. The critical density, $\rho_\mathrm{crit} = 3H_0/(8\pi G)$, where the present day Hubble constant $H_0 = 100\,h\,\mathrm{km\,s^{-1}\,Mpc^{-1}}$. n_s represents the spectral index of the primordial power-spectrum, and σ_8 denotes the *rms* linear mass fluctuation within a sphere of radius $8\,h^{-1}$Mpc extrapolated to $z = 0$. The simulations were carried out with an updated and extended version of the distributed-memory parallel TreeSPH code GADGET-2 (Springel 2005; Springel et al. 2001). Gravitational forces were computed using a combination of particle-mesh and tree algorithms. Hydrodynamic forces are computed with a variant of the smoothed particle hydrodynamics (SPH) algorithm that conserves energy and entropy where appropriate, i.e. outside of shocked regions (Springel & Hernquist 2002). Our simulations follow the radiative cooling of the gas, star formation, supernova feedback, and a photo-ionizing background (details can be found in Pfrommer et al. 2007). We model the cosmic ray (CR) physics in a self-consistent way (Pfrommer et al. 2006; Enßlin et al. 2007; Jubelgas et al. 2008). We include the adiabatic CR transport process such as compression and rarefaction, and a number of physical source and sink terms which modify the cosmic ray pressure of each CR population separately. The most important sources considered for injection are, diffusive shock acceleration at cosmological structure formation shocks and shock waves in supernova remnants, while the primary sinks are thermalization by Coulomb interactions, and catastrophic losses by hadronization. For simplicity, in this paper we do not take into account CRs injected into the inter-stellar medium from supernova remnants (see Pinzke, Oh, and Pfrommer, in prep. for a discussion of this topic).

⋆ e-mail:apinzke@physics.ucsb.edu (AP); peng@physics.ucsb.edu (PO);pfrommer@h-its.org (CP)

2.1 CR protons

The CR proton distribution function is given by

$$f_\mathrm{p}(p_\mathrm{p}) = \frac{\mathrm{d}^2 N_\mathrm{p}}{\mathrm{d}p_\mathrm{p}\,\mathrm{d}V} = C\,p_\mathrm{p}^{-\alpha}\,\theta(p_\mathrm{p} - q)\,, \tag{1}$$

and $p_\mathrm{p} = P_\mathrm{p}/m_\mathrm{p}c$, where we have normalized the proton momentum P_p with the proton mass m_p. Here q is the normalized momentum cutoff, α the spectral index, and C the normalization in units of density.

From our simulated galaxy clusters we derive for each snapshot at time t the injected CR proton distribution function f_p. We select particles in the outskirts of clusters where the gas densities are low and hence the Coulomb cooling of the CR protons small. The CR proton distribution function from the simulations is parameterized in terms of adiabatic invariant momentum cutoff q_0 and the adiabatic invariant Lagrangian amplitude of the spectrum $\tilde{C}_0$. We convert the adiabatic invariant quantities to physical quantities through

$$q = \left(\frac{\rho}{\rho_0}\right)^{\frac{1}{3}} q_0\,, \tag{2}$$

and

$$\tilde{C} = \left(\frac{\rho}{\rho_0}\right)^{-\frac{\alpha-1}{3}} \tilde{C}_0\,, \tag{3}$$

where the convenient unitless redefinition of the CR proton amplitude is given by

$$\tilde{C} = C\,m_\mathrm{p}/\rho\,. \tag{4}$$

The injected distribution function is calculated as the change in normalization between each snapshot, $f_\mathrm{inj,p}(p_\mathrm{p}) = \Delta C\,p_\mathrm{p}^{-\alpha}$, and is derived through the formalism developed in Enßlin et al. (2007) and Jubelgas et al. (2008):

$$\begin{aligned} \Delta C(t+\Delta t) &= C(t)\frac{\Delta\varepsilon_\mathrm{CR}(t) - T_\mathrm{p}(q(t))\,\Delta n_\mathrm{CR}(t)}{\varepsilon_\mathrm{CR}(t) - T_\mathrm{p}(q(t))\,n_\mathrm{CR}(t)}\,, \quad \text{where} \\ \Delta X(t) &= X(t+\Delta t) - X(t)\,. \end{aligned} \tag{5}$$

We fix the time between each snapshot Δt to 100 Myrs, which is smaller then the loss timescale of CR electrons in cluster outskirts. The CR proton number density is given by

$$n_{\rm CR} = \int_0^\infty {\rm d}p_{\rm p}\, f_{\rm p}(p_{\rm p}) = \frac{C\, q^{1-\alpha}}{\alpha - 1}\,, \quad (6)$$

provided $\alpha > 1$. The kinetic energy density of the CR proton population is

$$\varepsilon_{\rm CR} = \int_0^\infty {\rm d}p_{\rm p}\, f_{\rm p}(p_{\rm p})\, T_{\rm p}(p_{\rm p}) = \frac{C\, m_{\rm p}\, c^2}{\alpha - 1} \times \left[\frac{1}{2}\, {\rm B}_{\frac{1}{1+q^2}}\left(\frac{\alpha-2}{2}, \frac{3-\alpha}{2}\right) + q^{1-\alpha}\left(\sqrt{1+q^2} - 1\right)\right], \quad (7)$$

where $T_{\rm p}(p_{\rm p}) = (\sqrt{1+p_{\rm p}^2} - 1)\, m_{\rm p}\, c^2$ is the kinetic energy of a CR proton. ${\rm B}_x(a,b)$ denotes the incomplete Beta-function, and $\alpha > 2$ is assumed.

3 RADIO RELICS

RELICS... Collisionless cluster shocks are able to accelerate ions and electrons in the high-energy tail of their Maxwellian distribution functions through diffusive shock acceleration (for reviews see Drury 1983; Blandford & Eichler 1987; Malkov & O'C Drury 2001). Neglecting non-linear shock acceleration and cosmic ray modified shock structure, then electrons and protons are indistinguishable in the process of diffusive shock acceleration. There are, however, difference in: (1) the maximum energy of the steady state spectrum that depends on the details of the shock, (2) acceleration efficiency that is related to the smaller Larmor radius of the electrons that keeps the electrons from diffusing back and forth over the discontinuity of the shock front.CHECK

In this section we derive the CR electron distribution function by rescaling the injected CR proton spectrum to account for the different acceleration efficiencies as well as the shift in momentum due to the factor ~ 2000 difference in mass. In addition we model the Coulomb and radiative losses of the CR electrons.

3.1 CR electron distribution function

The injected CR electron distribution function at each time t is given by

$$f_{\rm inj,e}(p_{\rm e}) = \frac{{\rm d}^2 N_{\rm inj,e}}{{\rm d}V{\rm d}p_{\rm e}}(p_{\rm e}) = \frac{{\rm d}^2 N_{\rm inj,e}}{{\rm d}V{\rm d}p_{\rm p}}(p_{\rm e})\frac{m_{\rm e}}{m_{\rm p}} = \frac{{\rm d}^2 N_{\rm inj,p}}{{\rm d}V{\rm d}p_{\rm p}}(p_{\rm p})\left(\frac{p_{\rm e}}{p_{\rm p}}\right)^{-\alpha}\frac{\eta_{\rm max,e}}{\eta_{\rm max,p}}\frac{m_{\rm e}}{m_{\rm p}} = \Delta C\, p_{\rm e}^{-\alpha}\frac{\eta_{\rm max,e}}{\eta_{\rm max,p}}\frac{m_{\rm e}}{m_{\rm p}}\,. \quad (8)$$

and $p_{\rm e} = P_{\rm e}/m_{\rm e}c$, where we have normalized the electron momentum $P_{\rm e}$ with the electron mass $m_{\rm p}$. We use that maximal 50% of the energy available in a shock is injected into CR protons ($\eta_{\rm max,p}$) and a factor 10 smaller efficiency of 5% for the CR electrons ($\eta_{\rm max,e}$).

The CR electrons cool through inverse Compton (IC) emission and Coulomb losses on timescales that are relative short compared to the dynamical timescale of a cluster. We model these looses analytically by assuming a self similar solution for the CR electron distribution function (Sarazin 1999)

$$f_{\rm e}(\gamma_{\rm e}) \approx \frac{f_{\rm inj,e}(\gamma_{\rm e})}{\alpha - 1}\left(\frac{\gamma_{\rm low}}{\gamma_{\rm e}} + \frac{\gamma_{\rm e}}{\gamma_{\rm max}}\right)^{-1} \times \left\{2 - \left[\frac{1}{2}\left(1 - \frac{\gamma_{\rm e}}{\gamma_{\rm max}} + \left|1 - \frac{\gamma_{\rm e}}{\gamma_{\rm max}}\right|\right)\right]^{\alpha-1} - \left(1 + \frac{\gamma_{\rm low}}{\gamma_{\rm e}}\right)^{-(\alpha-1)}\right\}, \quad (9)$$

Here $\gamma_{\rm e} \approx p_{\rm e} = P_{\rm e}/m_{\rm e}c$ for $p_{\rm e} \gg 1$. The approximation in Eqn. (9) is valid as long as $\gamma_{\rm max} \gg \gamma_{\rm low}$, where the upper limit is determined from IC losses through

$$b_{\rm IC}(\gamma_{\rm e}) = b_{\rm IC}\gamma_{\rm e}^2 = \frac{4}{3}\frac{\sigma_{\rm T}}{m_{\rm e}c}U_{\rm cmb}\gamma_{\rm e}^2\,, \quad \text{and}$$
$$\gamma_{\rm max} = \frac{1}{b_{\rm IC}\,\Delta t}\,. \quad (10)$$

Here $\sigma_{\rm T} = 8\pi e^4/3(m_{\rm e}c^2)^2$ is the Thomson cross section and $U_{\rm cmb}$ is the energy density of the CMB in the cluster. The lower limit is determined from Coulomb losses through

$$b_{\rm C}(\gamma_{\rm e}) = b_{\rm C}\gamma_{\rm e}^2 = \frac{3\,\sigma_{\rm T}\, n_{\rm el}\, c}{2}\left[\ln\left(\frac{m_{\rm e}c^2\sqrt{\gamma_{\rm e}-1}}{\hbar\,\omega_{\rm plasma}}\right) - \ln(2)\left(\frac{1}{2} + \frac{1}{\gamma_{\rm e}}\right) + \frac{1}{2} + \left(\frac{\gamma_{\rm e}-1}{4\gamma_{\rm e}}\right)^2\right], \quad \text{and}$$
$$\gamma_{\rm low} = b_{\rm C}\,\Delta t\,. \quad (11)$$

Here $\omega_{\rm plasma} = \sqrt{4\pi e^2 n_{\rm e}/m_{\rm e}}$ is the plasma frequency, and $n_{\rm e}$ is the number density of free electrons.

We model the final CR electron spectrum as a superposition of five CR populations, each determined by Eqn. 9 but with a different spectral index and injected spectra.

3.2 Synchrotron emission

In this section we derive the synchrotron emission from the CR electron distribution. WORK UNDER PROGRESS

We fit the steady state CR electron distribution function in Fig. 1 with two power-laws

$$f_{\rm e,fit}(\gamma_{\rm e}) = C_1\,\gamma_{\rm e}^{-\alpha_1}\theta(\gamma_{\rm break} - \gamma_{\rm e}) + C_2\,\gamma_{\rm e}^{-\alpha_2}\theta(\gamma_{\rm e} - \gamma_{\rm break})\,. \quad (12)$$

The best fit CR electron normalization is given by $\mathbf{C} = (6 \times 10^{-4}, 10^7)$, the spectral index by $\alpha = (3.0, 5, 5)$, and the energy where the slope changes by $\gamma_{\rm break} = 1.2 \times 10^4$.

Probably need to calculate the emissivity numerically since there is a break in the power-law spectrum. Check We derive the radio synchrotron emissivity of the CR electrons from

$$J_0(\nu) \approx \left(\frac{e^2\,\nu_c}{c}\right)\sum_i C_i\Gamma\left(\frac{3\alpha_i - 1}{12}\right)\Gamma\left(\frac{3\alpha_i + 19}{12}\right)\frac{3^{\frac{\alpha_i}{2}}}{\alpha_i + 1}\left(\frac{\nu}{\nu_c}\right)^{\frac{1-\alpha}{2}}\,, \quad (13)$$

where the cyclotron frequency is given by $\nu_c = e\,B\,c/(2\pi m_{\rm e}c^2)$. We derive the total emitted power from the source by integrating the emissivity over the target volume. Here, we assume that the target volume have an uniform distribution of the CR electrons, hence the total power per unit frequency is given by

$$P_0(\nu) = \text{Volume} \times J_0(\nu)\,. \quad (14)$$

NEED TO REWRITE The size of a large relic is typically on Mpc scales, while the thickness is of the order 100 kpc and we assume that the relic along the line of sight is a Mpc, where the total radio emitting volume is about 0.1 Mpc^3. In addition we assume that the average magnetic field $B = 0.1\,\mu$G. The total emitted power at 1.4 PHz of the size typical for a large radio Relic is then given by $P_0(1.4\,{\rm PHz}) = 9 \times 10^{22}$ W/Hz. This is about a

factor 10-100 smaller than what is typically expected from a relic van Weeren et al. (2009). However, this luminosity is boosted by the shock or turbulence induced during a cluster merger. We follow the prescription outlined in Kang & Ryu (2011) to calculate the boost in radio luminosity due to reacceleration, and find that $P_2(1.4\,\mathrm{PHz}) \sim \times 10^{25}$ W/Hz in agreement with several of the relics listed in e.g. van Weeren et al. (2009).

OUTLINE THE PRESCRIPTION eq7, eq21

4 CONCLUSIONS

ACKNOWLEDGMENTS

REFERENCES

Blandford R., Eichler D., 1987, Phys. Rep., 154, 1
Drury L. O., 1983, Reports of Progress in Physics, 46, 973
Enßlin T. A., Pfrommer C., Springel V., Jubelgas M., 2007, A&A, 473, 41
Jubelgas M., Springel V., Enßlin T., Pfrommer C., 2008, A&A, 481, 33
Kang H., Ryu D., 2011, ApJ, 734, 18
Malkov M. A., O'C Drury L., 2001, Reports of Progress in Physics, 64, 429
Pfrommer C., Enßlin T. A., Springel V., Jubelgas M., Dolag K., 2007, MNRAS, 378, 385
Pfrommer C., Springel V., Enßlin T. A., Jubelgas M., 2006, MNRAS, 367, 113
Sarazin C. L., 1999, ApJ, 520, 529
Springel V., 2005, MNRAS, 364, 1105
Springel V., Hernquist L., 2002, MNRAS, 333, 649
Springel V., Yoshida N., White S. D. M., 2001, New Astronomy, 6, 79
van Weeren R. J., Röttgering H. J. A., Brüggen M., Cohen A., 2009, A&A, 508, 75

This paper has been typeset from a TEX/ LATEX file prepared by the author.

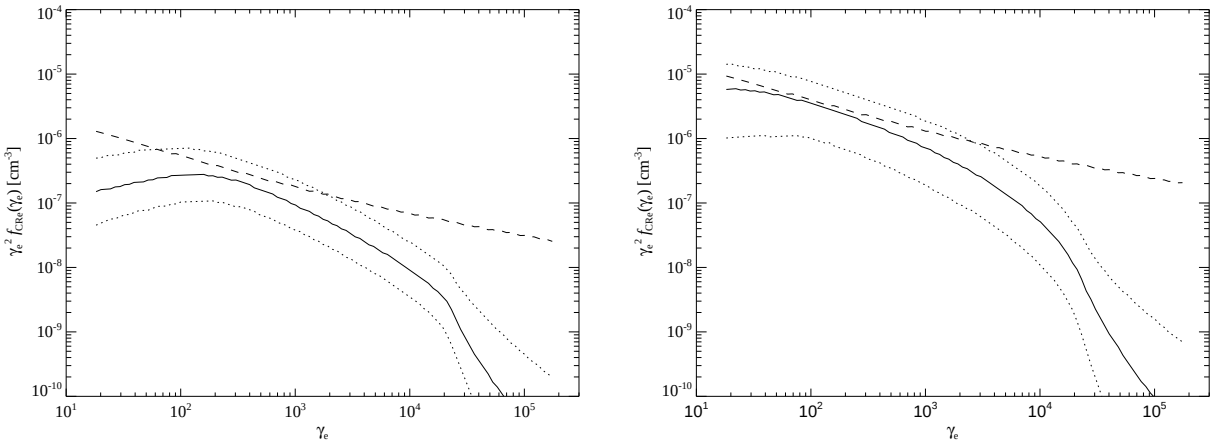

Figure 1. Cosmic ray electron spectra in cluster outskirts at redshift zero. We show the CR electron distribution function weighted with the electron Lorentz factor (γ_e) squared. In the *left panel* panel we show the CR electron in the region between (0.3-0.5)R_{200} and in the *right panel* between (1.3-1.5)R_{200}. The solid lines show the median CR electron spectrum where both radiative and adiabatic losses are included. The dotted lines shows the 68 percentiles. The dashed lines show the CR electron spectrum without Coulomb and radiative cooling. Note that the Coulomb cooling at low energies is very inefficient because of the low electron densities in the cluster outskirts.

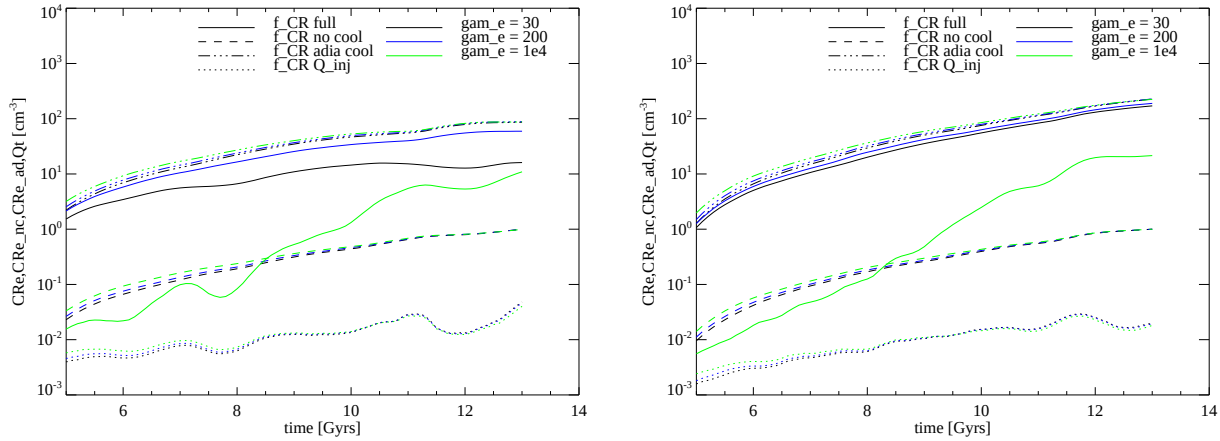

Figure 2. Time evolution of cosmic ray (CR) electron spectra. We show the CR electron distribution function weighted with the electron Lorentz factor (γ_e) squared. The time evolution of the CR electrons which at $z = 0$ reside from (0.3-0.5)R_{200} are shown in the *left panel* and (1.3-1.5)R_{200} in the *right panel*. The black lines show the CR electrons with a $\gamma_e = 30$, blue lines $\gamma_e = 200$, and green lines $\gamma_e = 10^4$. The solid lines show the CR electrons with full cooling, i.e. for Coulomb, inverse Compton, and adiabatic losses. Dashed lines show the CR electrons without Coulomb and inverse Compton cooling while the dash-dotted lines show the CR electrons without adiabatic cooling. The dotted line show the injected CR electron distribution function, derived from the injected CR protons. For each energy, we normalize the CR electron distribution function with the CR electrons without cooling. Notice that the high energy part is built up during the last Gyr. This is explained by the inverse Compton losses that are larger at high energies, especially at high redshifts where the energy density of the CMB is much larger than today.

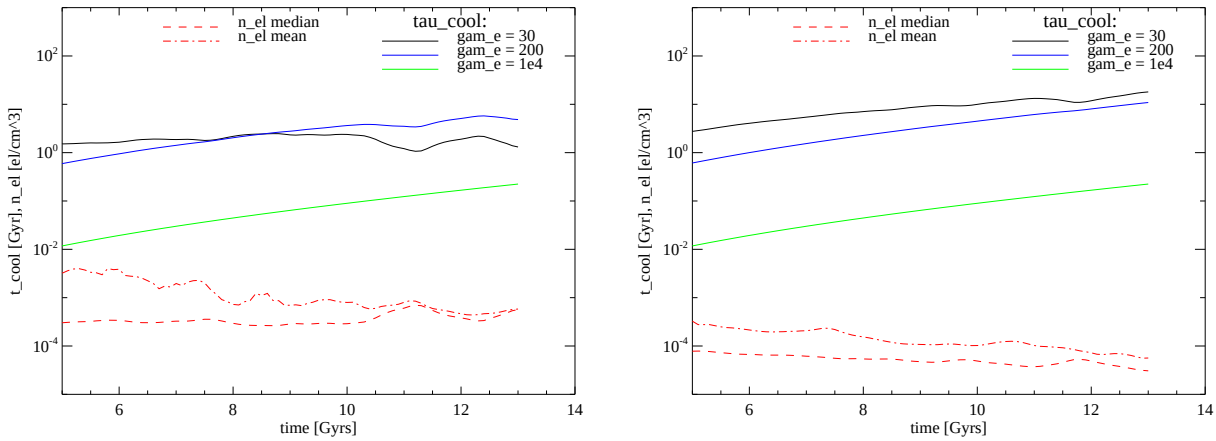

Figure 3. Time evolution of the gas density and the cosmic ray (CR) cooling time. We show the time evolution of the electron number density and CR electron cooling time that are associated with the CR electrons which at redshift $z = 0$ reside from (0.3-0.5)R_{200} in the *left panel* and (1.3-1.5)R_{200} in the *right panel*. The red lines show the electron number densities, where the dashed line show the median and dash-dotted the mean. The solid lines show the cooling times $\tau_{\rm cool} = \gamma_{\rm e}/[b_{\rm IC}(\gamma_{\rm e}) + b_{\rm C}(\gamma_{\rm e})]$ for $\gamma_{\rm e} = 30$ (black), $\gamma_{\rm e} = 200$ (blue), and $\gamma_{\rm e} = 10^4$ (green). Interesting the CR cooling at low energies of the particles that end up in the center is constant while is increasing monotonically for the particles that end up in the cluster periphery. The density of the particles that end up in the center is roughly constant with time while it is decreasing for the particles that end up in the outer part. This is due to the expansion of the universe that counteract the contraction of the particles in the cluster periphery.